RR 302

Research Report 302

MEASUREMENTS OF LASER EXTINCTION IN ICE FOG FOR DESIGN OF SEV PILOTAGE SYSTEM

Richard Munis and Allan Delaney

August 1972

CORPS OF ENGINEERS, U.S. ARMY
COLD REGIONS RESEARCH AND ENGINEERING LABORATORY
HANOVER, NEW HAMPSHIRE

R
24

DOCUMENT CONTROL DATA - R & D

(Security classification of title, body of abstract and indexing annotation must be entered when the overall report is classified)

1. ORIGINATING ACTIVITY (Corporate author)
U.S. Army Cold Regions Research and Engineering Laboratory
Hanover, New Hampshire 03755

2a. REPORT SECURITY CLASSIFICATION
Unclassified

2b. GROUP

3. REPORT TITLE
MEASUREMENTS OF LASER EXTINCTION IN ICE FOG FOR DESIGN OF SEV PILOTAGE SYSTEM

4. DESCRIPTIVE NOTES (Type of report and inclusive dates)

5. AUTHOR(S) (First name, middle initial, last name)
Richard Munis and Allan Delaney

6. REPORT DATE	7a. TOTAL NO. OF PAGES	7b. NO. OF REFS
August 1972	~~26~~ 24	7

8a. CONTRACT OR GRANT NO.
ARPA Order 1615

b. PROJECT NO.

c.

d.

9a. ORIGINATOR'S REPORT NUMBER(S)
Research Report 302

9b. OTHER REPORT NO(S) (Any other numbers that may be assigned this report)

10. DISTRIBUTION STATEMENT
Approved for public release; distribution unlimited.

11. SUPPLEMENTARY NOTES

12. SPONSORING MILITARY ACTIVITY
Advanced Research Projects Agency

13. ABSTRACT

Laser extinction measurements in ice fog were made at wavelengths of 0.6328, 1.15 and 3.39 μ. The ice fog was generated in an environmental chamber whose temperature could be lowered to -43°C. Particle sampling was carried out simultaneously with the laser measurements using an impactor. Size distributions were derived from the impactor measurements. These data were used to compute Mie extinction coefficients at the three laser wavelengths. These coefficients were compared with the coefficients derived experimentally. Although some discrepancy exists between theory and experiment, both agree fairly well on the behavior of the extinction coefficient as a function of particle concentration.

14. Key Words
- Air cushion vehicle
- Ground effect vehicle
- Helium-neon laser measurements
- Optical properties of ice fog
- Surface effect vehicle
- Terrain avoidance systems

DD FORM 1 NOV 68 1473 REPLACES DD FORM 1473, 1 JAN 64, WHICH IS OBSOLETE FOR ARMY USE.

MEASUREMENTS OF LASER EXTINCTION IN ICE FOG FOR DESIGN OF SEV PILOTAGE SYSTEM

Richard Munis and Allan Delaney

August 1972

PREPARED FOR
ADVANCED RESEARCH PROJECTS AGENCY
ARPA ORDER 1615
BY
CORPS OF ENGINEERS, U.S. ARMY
COLD REGIONS RESEARCH AND ENGINEERING LABORATORY
HANOVER, NEW HAMPSHIRE

I-15

PREFACE

This report was prepared by Dr. Richard Munis, Research Physicist, and Mr. Allan Delaney, Physical Science Technician, of the Research Division, U.S. Army Cold Regions Research and Engineering Laboratory (USA CRREL).

This work was done under Advanced Research Projects Agency Order 1615.

Mr. Leonard Stanley, Technical Services Division (TSD), wrote the computer program to calculate the Mie extinction coefficients for this study. Mr. Robert Demars, TSD, provided photographic support.

CONTENTS

ILLUSTRATIONS

TABLES

MEASUREMENTS OF LASER EXTINCTION IN ICE FOG FOR DESIGN OF SEV PILOTAGE SYSTEM

by

Richard Munis and Allan Delaney

INTRODUCTION

The operation of any vehicle during conditions of low visibility requires that the operator be able to "see" through various weather conditions, including fog, rain and snow. The operation of the vehicle on arctic terrain in addition requires that the operator be prepared to avoid ridges on sea ice. This combination of problems must be considered in the design of an obstacle avoidance system for a surface effect vehicle (SEV).

The Advanced Research Projects Agency (ARPA) has initiated a program on electromagnetic propagation to study the effects on vehicle operation of snow and ice covered terrain, and ice and water fog at visible, infrared, millimeter, and microwave wavelengths. As part of this program, a report has been prepared on the radar cross-section measurements of snow and ice.[2] The purpose of the present report is to present data on laser extinction measurements in ice fog at wavelengths of 0.6328, 1.15 and 3.39 μ.

LITERATURE REVIEW

A great deal of effort has been spent in studying the mechanism of ice fog formation. In 1954, Thuman and Robinson[5] made the first observations of the size distribution of ice fog crystals near Fairbanks, Alaska. In 1964, Kumai[3] prepared a report on the concentration and size distribution measurements of ice fog also in the vicinity of Fairbanks. Most recently, Benson[1] and Weller[7] summarized the results of these investigations of the Fairbanks ice fog and Ohtake[4] attempted to confirm the mechanism of ice fog formation that he and other investigators had previously postulated.

According to Ohtake,[4] the primary sources of ice fog in the Fairbanks area were open water, and automobile and heating plant exhaust. One might at first question whether such sources of ice fog would be significant to a SEV operating in arctic regions, well away from the influence of city environments; however, it is quite possible that ice fog would form on nuclei from the SEV exhaust. Thus, any suitably designed obstacle avoidance system for the SEV should be provided with the capability of detecting obstacles through low-visibility conditions generated by the vehicle itself.

Although much theoretical and experimental research has been done on the scattering and absorption properties of warm fog, very little work has been done on the extinction properties of ice fog. One significant reason for the lack of data may be the difficulty of producing ice fog in the laboratory. Another may be the problem of obtaining field data at temperatures as low as -40°C.

Regardless of the reason, the present investigation is not based on the extensive experience of other workers. The various problems confronting the researcher who attempts to make meaningful extinction measurements in ice fog and to relate them to existing theory are discussed in Appendix A.

EXPERIMENTAL PROCEDURE

The extinction measurements at 0.6328, 1.15 and 3.39 μ were made in a 4-m-long fog chamber located in a coldroom whose temperature could be lowered to approximately –36°C. Temperatures below –40°C were achieved inside the fog chamber by cooling coils located inside the chamber. Figure 1 shows an exterior view of this chamber and Figure 2 shows the optical path down which the laser beam was propagated toward the detector. Figure 3 shows the interior of the room in which the helium-neon laser and the electronic processing equipment were located. The temperature of this room was kept at approximately 20°C.

The extinction measurements were made in the following manner. The modulated laser beam was sampled at the opposite end of the 4-m fog chamber by a photodiode and the signal obtained was processed by a lock-in amplifier before being recorded. The strip chart recorder was allowed to run long enough to establish a stable signal level. This signal level was then used as a measure of the incident radiation impinging upon the fog.

Following this, a fog was produced in the chamber by using a technique that is discussed in Appendix B. As the attenuation of the laser beam was continuously recorded, fog particles were sampled with an impactor (Fig. 4). The fog concentration varied over a rather wide range while the beam attenuation was being measured. Immediately after the fog particles were sampled, the glass slide was removed from the impactor, placed under a microscope and photographed. Figures C1a-C7a, Appendix C, show ice fog samples taken during these experiments. Photographs of these samples were later enlarged to obtain particle spectra. Figures C1b-C7b show the corresponding plots of diameter d vs number of particles N for each of the ice fog samples.

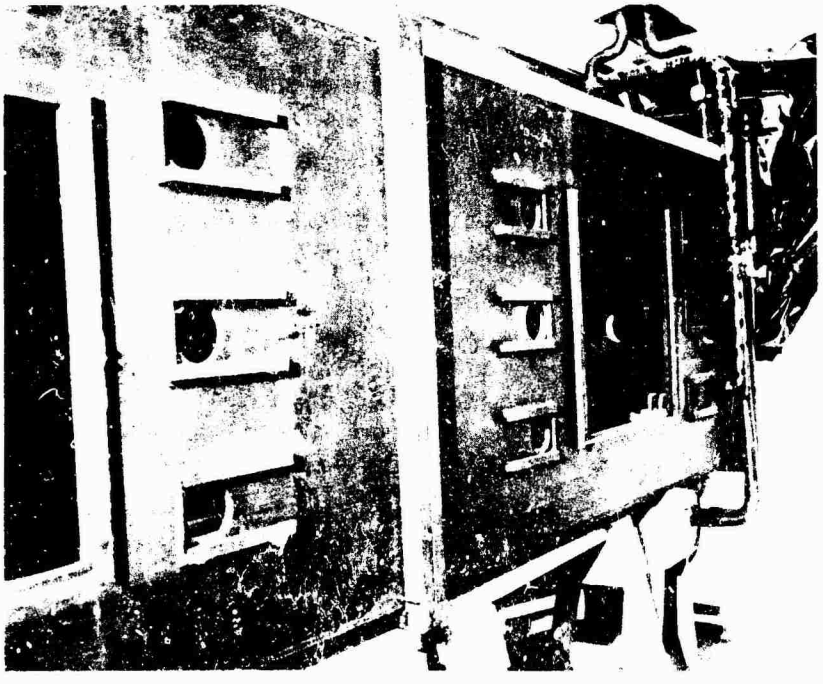

Figure 1. Exterior view of fog chamber. Ice fog samples are obtained by inserting the impactor into one of the circular ports.

Figure 2. Optical path of the laser propagation. Overhead pipes bring –75°C brine into the chamber.

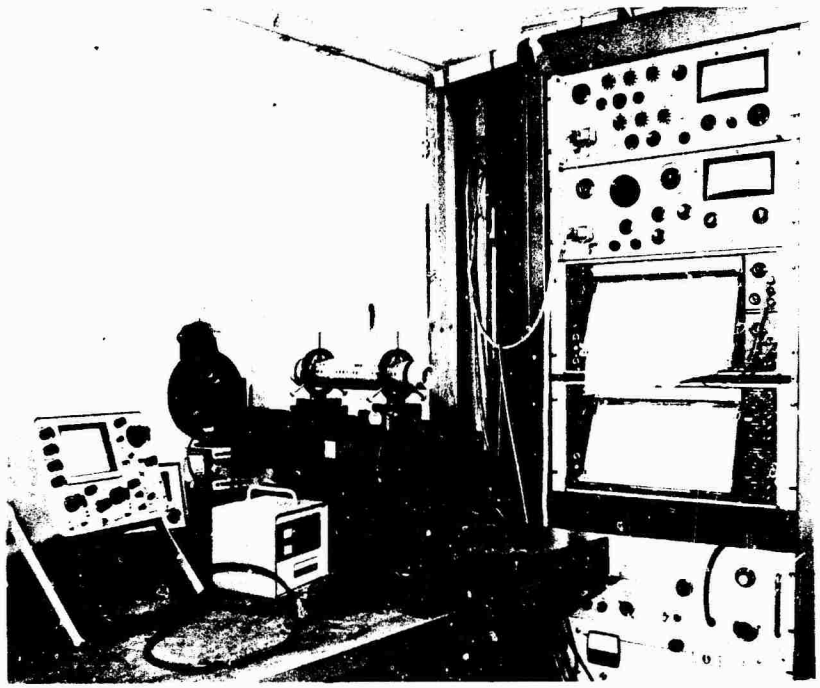

Figure 3. Interior of room containing helium-neon laser and electronic processing equipment.

Figure 4. Impactor with which fog samples were obtained. As a measured volume of air is drawn through an orifice by pulling back the syringe, ice fog particles contained in the air sample are deposited in a film of silicone oil on a microscope slide located underneath the orifice.

EXPERIMENTAL AND THEORETICAL EQUATIONS

The extinction coefficient at each wavelength λ for each particle concentration N may be calculated according to

$$T(\lambda, N) = e^{-\alpha(\lambda, N)\ell} \tag{1}$$

where

$T(\lambda, N)$ = measured transmission (%)

ℓ = optical path length (m)

$\alpha(\lambda, N)$ = extinction coefficient (m^{-1}).

The extinction coefficient for a single particle may be written as:[6]

$$\alpha = S + A \tag{2}$$

where

S = scattering coefficient (m^{-1})

A = absorption coefficient (m^{-1}).

At a wavelength of 0.6328 μ absorption is insignificant because most of the radiation not impinging upon the detector is lost only to angular scattering out of the primary beam. However, at 3.39 μ both terms in eq 2 contribute to the loss of radiation as the beam traverses the fog chamber. Thus, at this wavelength the complex part of the index of refraction becomes a significant factor in calculating the theoretical extinction coefficient.

The magnitude of the theoretical extinction coefficient may be calculated from the particle size distribution and the Mie theory using the relation[6]

$$\gamma = \sum_{a_{min}}^{a_{max}} N(a)\, \Delta a \pi a^2 Q_{ext}(m, x) \tag{3}$$

where

$N(a)$ = particle concentration per Δa radius interval

πa^2 = geometrical cross-section area of a single particle

Q_{ext} = van de Hulst's dimensionless efficiency factor for total extinction[6]

m = complex index of refraction

x = particle size parameter $2\pi a/\lambda$.

Equation 3 is rigorously valid only for single scattering caused by spherical particles.

RESULTS AND DISCUSSION

Table I compares the theoretical and experimental extinction coefficients of ice fog at 0.6328 μ computed from eq 1 and 3. Also included are the total particle concentration of each sample and the measured value of transmission. The last column of this table gives the attenuation in terms of db/m, a value that is probably more useful to the systems designer.

Table I. Experimental and theoretical extinction coefficients of ice fog at 0.6328-μ and –36°C.

Particle concentration (N/cm^3)	*Experimental extinction coefficient* (m^{-1})	*Mie extinction coefficient* (m^{-1})	*Transmission* (%)	*Attenuation* (db/m)
66	0.0320	0.0212	88	–0.0138
20	0.0496	0.0095	82	–0.0215
15	0.0621	0.0126	78	–0.0268
108	0.1236	0.0268	61	–0.0534

Figure 5 shows the behavior of the experimental extinction coefficient at 0.6328 μ as the particle concentration increases and the predicted behavior of the extinction coefficient according to Mie theory. Although there is some disagreement between theory and experiment, both indicate the same behavior as particle concentration increases; that is, after a certain particle concentration has been attained asymptotically no further increase of the extinction takes place. During this set of measurements the authors experienced significant difficulty in generating a repeatable ice fog; therefore, these data had to be assembled from two different fog samples. Fig. C1a and C1b show the fog sample and the corresponding particle spectra for one of these samples.

Tables II and III give the experimental and theoretical extinction coefficients of ice fog at 1.15 μ and 3.39 μ respectively for a chamber temperature of –43°C. Figures 6 and 7 show the behavior of the two coefficients as the particle concentration increases. At 1.15 μ the agreement between the two is relatively good. However, the most striking aspect of this comparison is that both experiment and theory indicate a change of the rate of extinction at about 90 particles/cm^3. At this value a new rate is established and both experiment and theory show approximately the same general trend for the available data. By this time the problem of generating a repeatable fog had been overcome; thus these data are from samples taken from one fog as it dissipated.

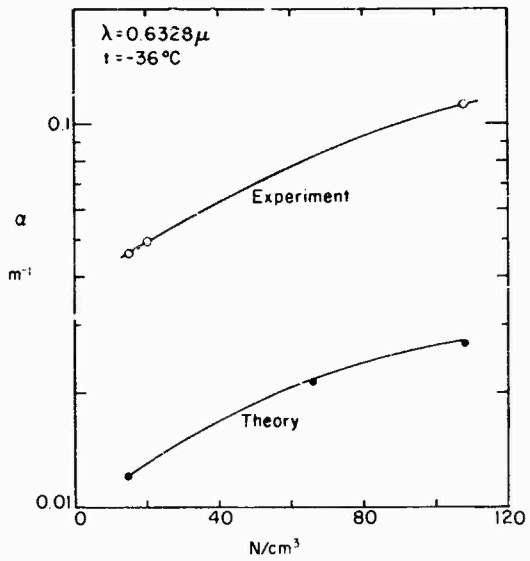

Figure 5. Experimental and theoretical extinction coefficients as particle concentration increases at 0.6328 μ.

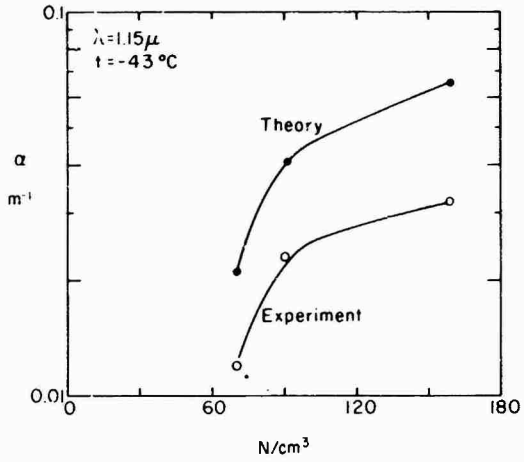

Figure 6. Experimental and theoretical extinction coefficients as particle concentration increases at 1.15 μ.

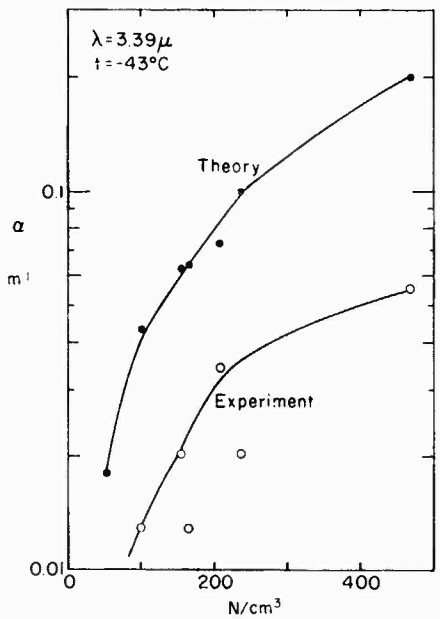

Figure 7. Experimental and theoretical extinction coefficients as particle concentration increases at 3.39 μ.

Table II. Experimental and theoretical extinction coefficients of ice fog at 1.15 μ and –43°C.

Particle concentration (N/cm^3)	Experimental extinction coefficient (m^{-1})	Mie extinction coefficient (m^{-1})	Transmission (%)	Attenuation (db/m)
70	0.0128	0 0214	95	–0.0055
91	0.0234	0.0401	91	–0.0102
159	0.032	0.0649	88	–0.0138

Table III. Experimental and theoretical extinction coefficients of ice fog at 3.39 μ and –43°C.

Particle concentration (N/cm^3)	Experimental extinction coefficient (m^{-1})	Mie extinction coefficient (m^{-1})	Transmission (%)	Attenuation (db/m)
54	0.0075	0.0182	97	–0.00324
165	0.0128	0.0641	95	–0.0055
101	0.0128	0.0432	95	–0.0055
238	0.0207	0.1024	92	–0.00895
155	0.0207	0.0628	92	–0.00895
209	0.0348	0.0731	87	–0.0150
469	0.0557	0.2027	80	–0.024

Figure 8 shows a composite plot of the particle spectra at sampling times t_0, t_1 and t_2. At t_0 the peak of the distribution was located at 15.2 μ, at t_1 it had shifted slightly to 14.4 μ, and at t_2 a significant shift located it at 11.6 μ. Figure 8 also shows that at t_0 the particle concentration was 165/cm^3, but when it had reached 91/cm^3 the spectrum shifted such that there were fewer particles and the mean particle size was getting smaller. At this point the rate of extinction suddenly increased and the mean diameter of the particle shifted again to an even smaller size. It is not possible at this time to determine whether the extinction coefficient at 70/cm^3 was smaller than that at 165/cm^3 because the number of particles was smaller or because the mean diameters of the particles were smaller.

Figure 9 shows a composite plot of the particle spectra taken during the experimental work at 3.39 μ. Here a different distribution-time relationship evolved; that is, the particle spectrum first shifted to a larger mean size before it shifted back again to the original distribution, where it remained unchanged until the fog dissipated. Figure 10 shows a plot of concentration versus extinction coefficient for the data samples obtained during the same fog. Unfortunately agreement between theory and experiment was not as remarkable as at 1.15 μ.

Figure 11 plots the experimental extinction coefficient in units of db/m versus particle concentration at the three laser wavelengths. Again, it must be emphasized that more than one particle

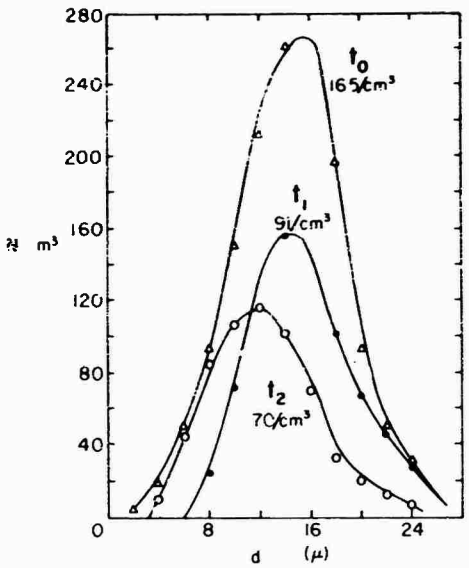

Figure 8. Particle spectra at sampling times t_0, t_1, and t_2.

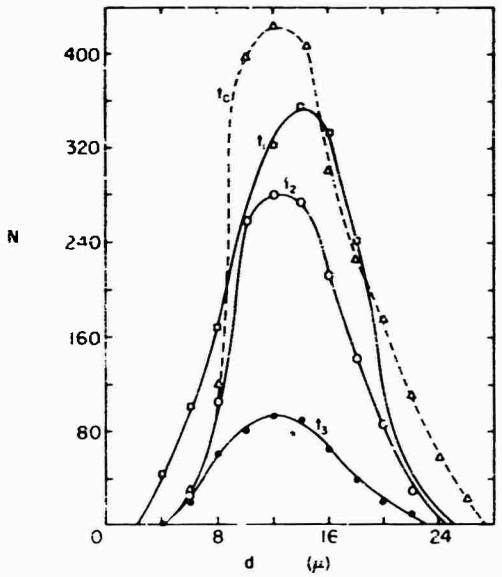

Figure 9. Particle distribution measured as fog dissipated.

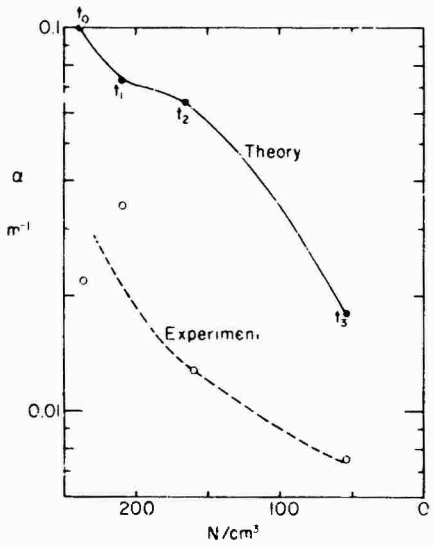

Figure 10. Experimental and theoretical extinction coefficients versus particle concentration at 3.39 μ.

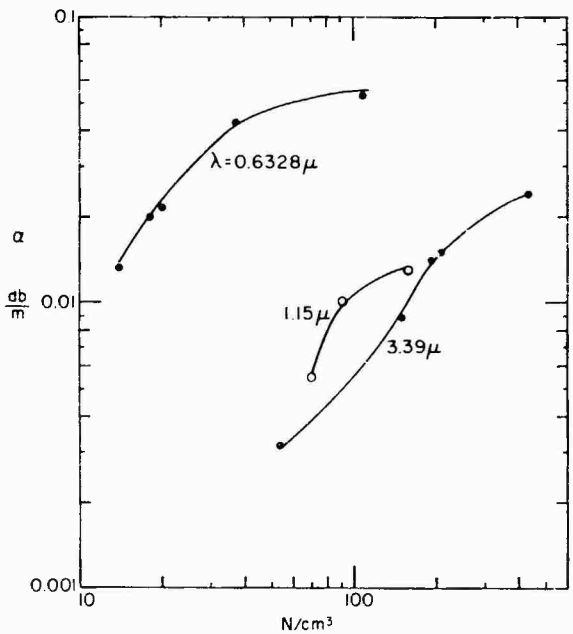

Figure 11. Experimental extinction coefficient versus particle concentration for three laser wavelengths.

size distribution is represented by these data. However, the important feature here is the comparison at these three wavelengths of the attenuation properties of ice fog of varying concentration. From Figure 11 we may deduce that at 0.6328 μ only a few particles per cm^3 cause an appreciable loss of energy in the form of scattering. However, at the two infrared wavelengths (1.15 μ and 3.39 μ) the same concentration causes only a negligible loss of energy. Further inspection shows that in extremely dense fogs loss of energy becomes appreciable at 3.39 μ, whereas at 1.15 μ it appears from the available data that the extinction coefficient does not rise as rapidly as it does at 3.39 μ. This seems to agree with the fact that the imaginary part of the index of refraction of ice is about 10^4 higher at 3.39 μ than at 1.15 μ.

CONCLUSIONS

Experimental and theoretical data have been presented for three laser wavelengths: 0.6328, 1.15 and 3.39 μ. The authors experienced a good deal of difficulty at the beginning of the program in generating and obtaining good ice fog samples. However, these problems have been largely overcome and it is now possible to generate repeatable fogs. The results of this study have shown that there is generally fairly good agreement between the experimentally derived extinction coefficients and those predicted by the Mie theory. More remarkable is the fact that at 1.15 μ experiment and theory show excellent agreement between the behavior of the extinction coefficient and particle concentration. However, more data are needed at both lower and higher particle concentrations to substantiate the agreement between theory and experiment.

LITERATURE CITED

1. Benson, C.S. (1970) Ice fog: Low temperature air pollution defined with Fairbanks, Alaska as type locality. USA CRREL Research Report 121.

2. Hoekstra, P. and D. Spanogle (1971) Radar cross-section measurements of snow and ice for design of SEV pilotage system. U.S. Army Cold Regions Research and Engineering Laboratory (USA CRREL) Internal Report 175.

3. Kumai, M. (1964) A study of ice fog and ice fog nuclei at Fairbanks, Alaska, Part I. USA CRREL Research Report 150 (AD 451667).

4. Ohtake, J. (1970) Studies on ice fog. University of Alaska Geophysical Institute, Report UAGR-211.

5. Thuman, W.C. and E. Robinson (1954) Studies of Alaskan ice-fog particles. *Journal of Meteorology*, vol. 11, p. 151-56.

6. Van de Hulst, H.C. (1957) *Light scattering by small particles.* New York: John Wiley and Sons, Inc.

7. Weller, G. (1969) Ice fog studies in Alaska. University of Alaska Geophysical Institute, Report UAGR-207.

APPENDIX A: SOME PROBLEMS IN THE EXPERIMENTAL DETERMINATION OF THE EXTINCTION COEFFICIENT OF ICE FOG

Recently the difficulty of reliably characterizing an ice fog distribution by particle size and number has been markedly reduced. The viscosity of oil used to collect ice particles is very important in determining any distribution because if the oil is too thin and large particles are sampled it cannot support the momentum of the particles as they impact on the slide and they therefore crash into the slide and disintegrate.

However, even if proper oil viscosity is selected success cannot be guaranteed because the problem of *depositing* the oil on the slide still remains. If care is not taken to restrict the oil from spreading too much after it is deposited, the particles still tend to disintegrate because of the "thinness" of the oil deposit rather than the viscosity. The authors conducted a series of tests in which the same viscosity of oil was deposited in a slightly different manner. If extreme care was not taken a variation of up to 400% could be expected in the total number of particles collected on the slide. Even with extreme care variations of between 10-50% were observed. Clearly this problem must be given more attention if better agreement is to be obtained between theory and experiment.

Another problem has recently come to the authors' attention: if a rather small aperture is used on the impactor to admit the fog particles and if the syringe is spring-loaded, the velocity with which the air enters the sample chamber is so high that it causes the oil to separate, thus allowing the particles to crash into the glass slide and disintegrate. However, releasing the syringe slowly prevents this problem and makes it possible to obtain rather consistent results.

APPENDIX B: ICE FOG PRODUCTION TECHNIQUE

The fog production technique uses a pressure cooker to produce steam which is then sprayed directly into the fog chamber until the chamber is saturated. Ice crystals begin to form almost as soon as the steam starts to cool down to the chamber temperature. At this point the fog is "moved" around in the chamber until it is thoroughly mixed. The reason for this is that since the steam is admitted into the chamber at only one location the laser propagation path tends to have a more random fog particle distribution along the complete length of the path than if the fog were permitted to spread from its initial position. After the fog has been stirred about it is then permitted to dissipate without any further interferences. As it dissipates samples are taken and photographed approximately every 2-3 min until it is completely dissipated; this is done in conjunction with the continuous recording of the laser beam attenuation.

The authors have been greatly encouraged by the close resemblance of the fog samples taken during this investigation to those obtained by Ohtake in Fairbanks, Alaska.[4] Figure B1 shows the range of the mean diameter d_m of spherical ice particles versus temperature for samples taken during this investigation, and Figure B2 shows the data of Ohtake[4] and Thuman and Robinson[5] taken in Alaska. A comparison of these results indicates that the technique for generating ice fog in the environmental chamber used in the present investigation is indeed realistic.

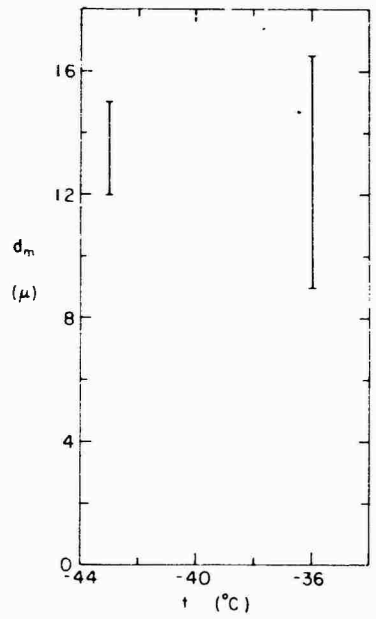

Figure B1. Mean diameter of spherical ice particles versus temperature.

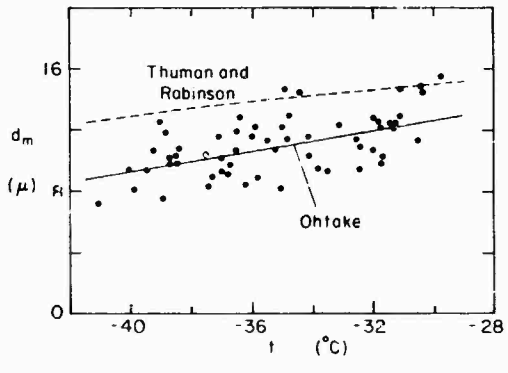

Figure B2. Mean diameter of spherical ice particles versus temperature.[4]

APPENDIX C: ICE FOG SAMPLES AND THEIR CORRESPONDING PARTICLE SPECTRA

(N = number of particles and d = diameter of ice fog sample.)

C1a.

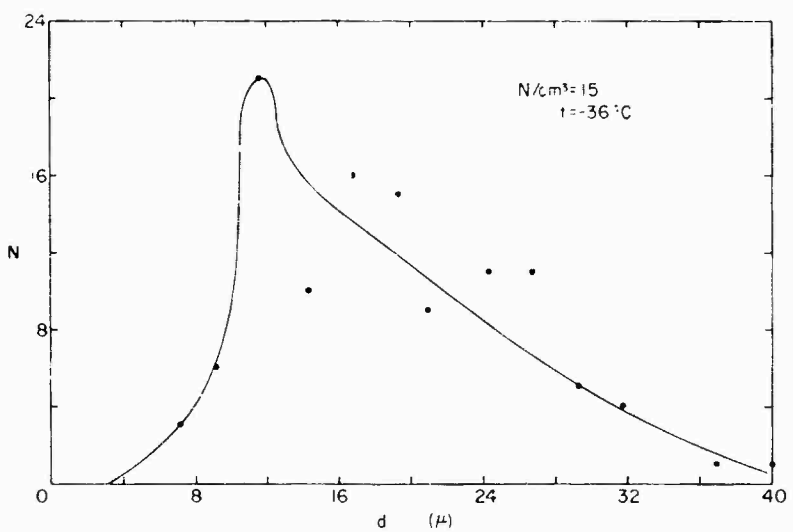

C1b.

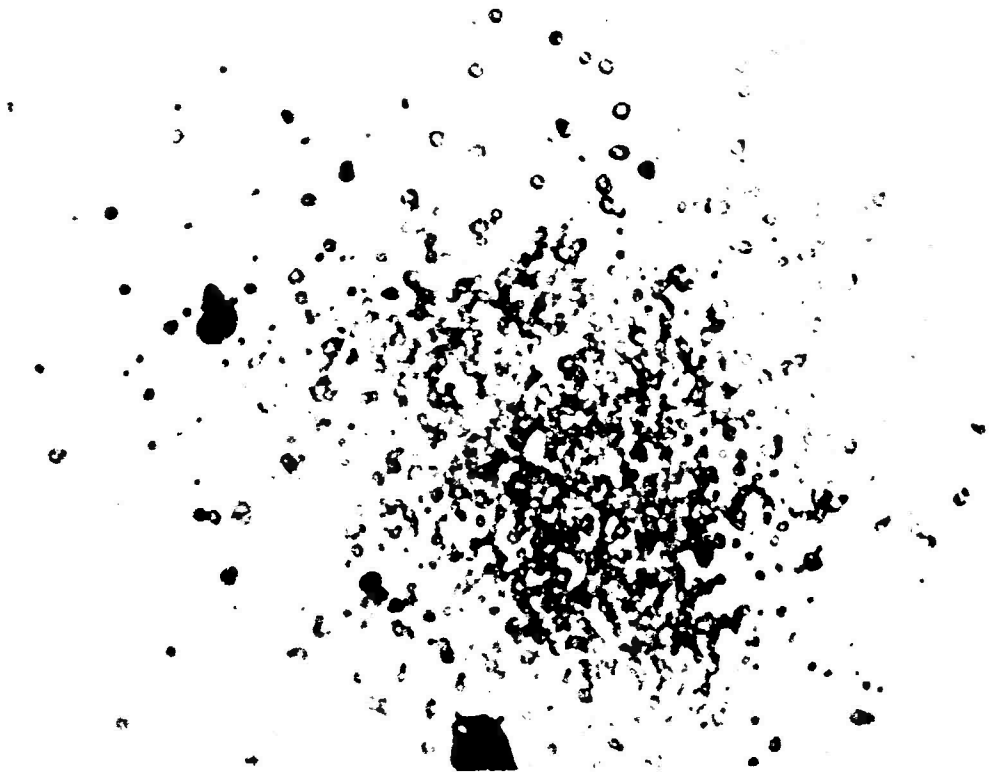

C2a.

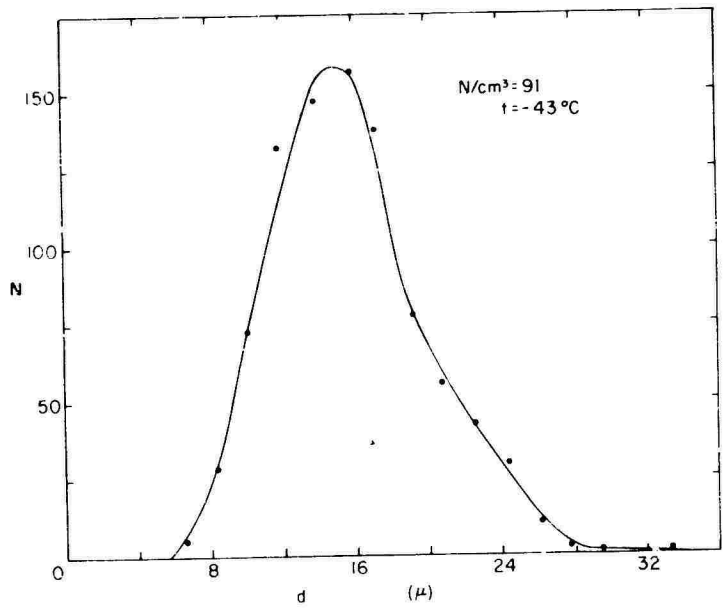

C2b.

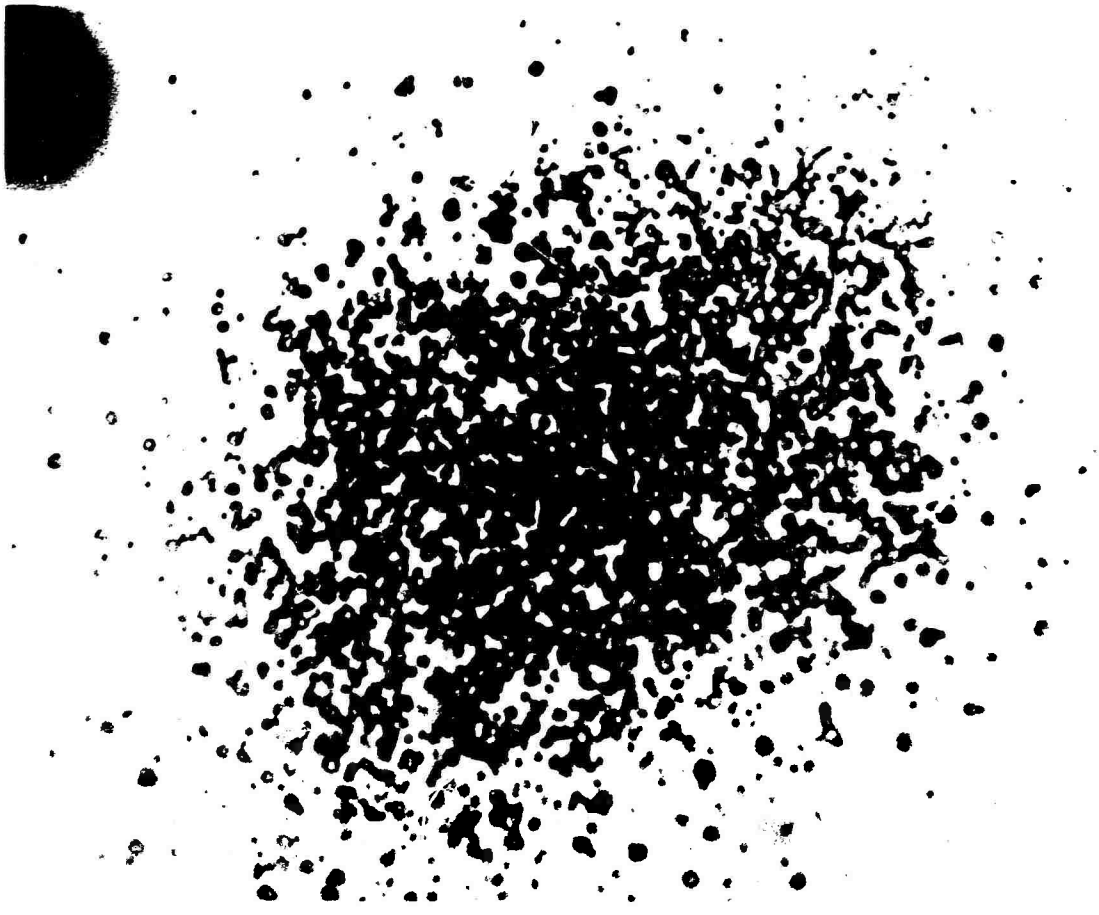

C3a.

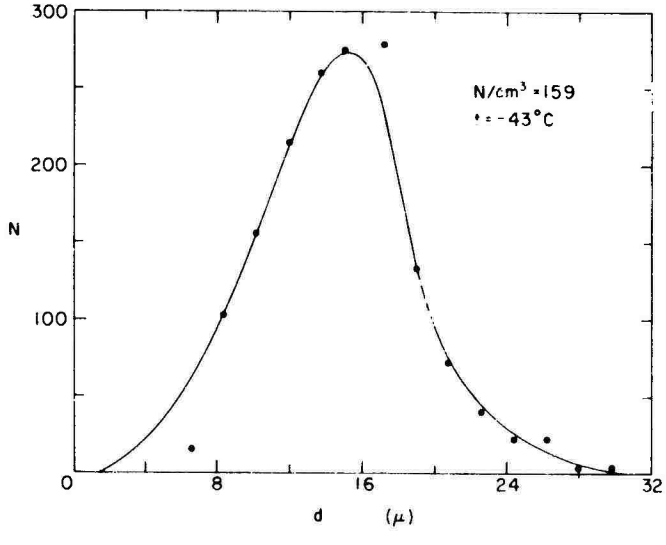

C3b.

C4a.

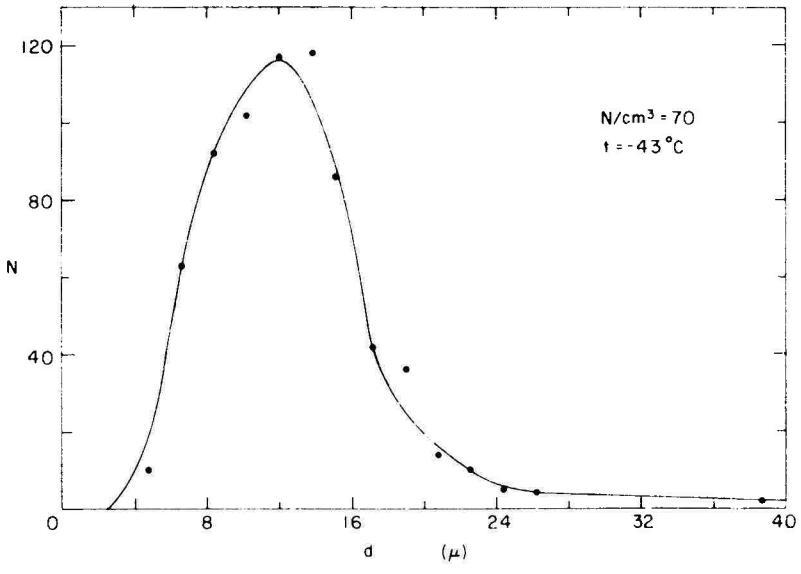

C4b.

C5a.

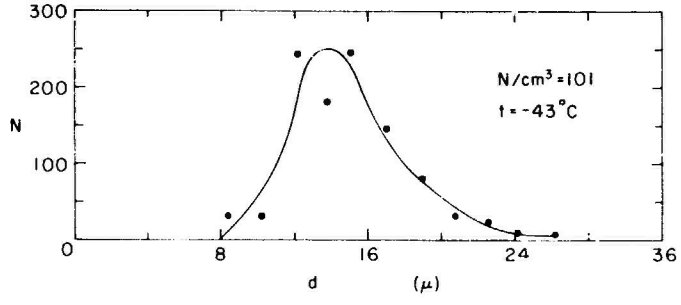

C5b.

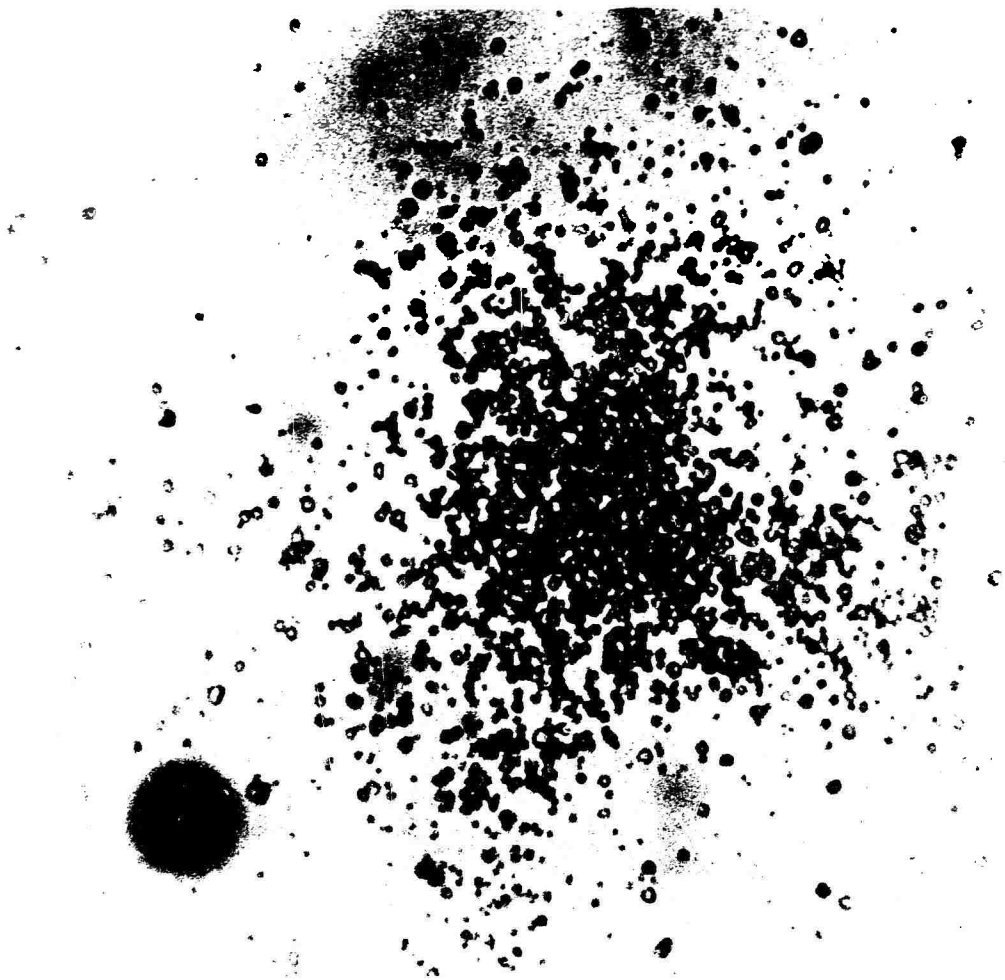

C6a.

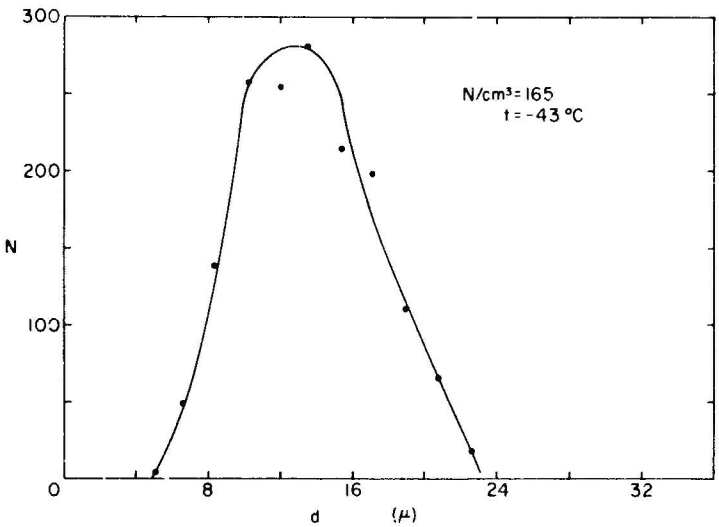

C6b.

C7a.

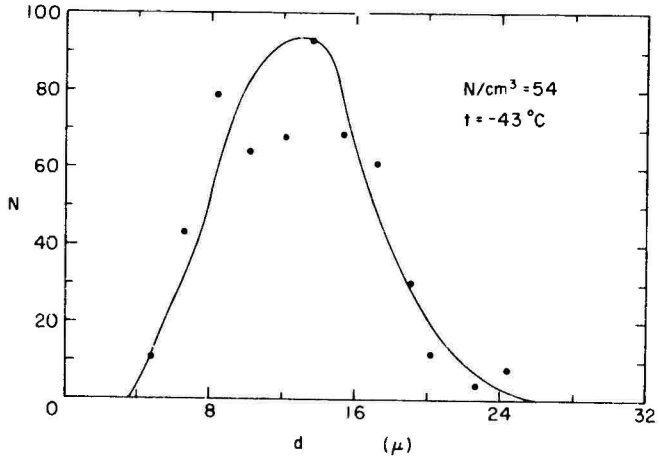

C7b.